

# Spectrally Selective Transformations of Solar Radiation by Retinal Photoreceptors in the Control of the Circadian Rhythm of the Human Body throughout an 11-Year Cycle of Solar Activity

A. V. Leonidov\*

*Biophysics, ul. Butlerova 17b, Moscow, 117342 Russia*

*\*e-mail: avleonidoff@mail.ru*

Received May 21, 2019; revised May 21, 2019; accepted December 25, 2019

**Abstract**—The round-the-day effect of solar radiation on photoreceptors of the retina of the eye and its role in the control of the circadian rhythm of the human body within an arbitrary 11-year cycle of solar activity are considered. Processed data describing the variation of the spectral and energy characteristics of solar radiation that reach the Earth's surface over a solar activity cycle are given. On this basis, a generalized analytical expression has been obtained that models the spectrally selective processing of the sum of the direct and diffuse components of solar radiation by retinal rods and blue-sensitive (S type) cones. The obtained expression allows consideration of separate spectrally selective processing of the direct and diffuse components of solar radiation by rods and S cones of retina, including the case of a catastrophic lesion of one of the neuronal paths that connect rods or S cones with suprachiasmatic hypothalamus nuclei. It is shown that the effective spectrum obtained as a result of spectral selection of the components of solar radiation that is used to control the circadian activity of the human body is determined solely by the spectral sensitivity of rods and S cones. The effective spectrum does not depend on daily variations in the spectrum of solar radiation as the angular elevation of the Sun varies; the daily energy characteristics of the effective spectrum, which vary within each solar activity cycle, retain their dependence on the Sun's elevation in the daytime and on the current phase of the solar activity cycle. Significant changes in the characteristics of solar radiation within the cycle of solar activity infer that it is necessary to take them into account in studying and modeling the control processes of human circadian activity driven by solar radiation.

**Keywords:** circadian activity, rods, S cones, retina, relative spectral circadian efficiency, spectral selection, solar activity cycle, radiation, atmospheric transmission coefficients, spectral density of irradiance, irradiance

**DOI:** 10.1134/S0006350920030124

The circadian variation of indices of natural irradiance of the terrestrial surface produced by solar radiation is the main physical factor that controls the circadian activities of the entire human body [1]. This variation is also affected by the clear 11-year solar activity cycle, which is also known as the Schwabe cycle [2–4]. The cyclic variation in solar activity, associated with the number of sunspots (Wolf number  $W$  [2]) on the apparent surface of the photosphere of the Sun, causes cyclic changes in the effective absolute temperature  $T_{\text{eff}}$  of solar radiation, the absolute indices of the spectral density of photosphere luminance, and photosphere luminance itself. The maximum amplitudes of photosphere luminance indices within one solar activity cycle can reach approximately 35%. Obviously, these changes affect the control and indices of human circadian activities in any phase of the solar cycle.

*Abbreviations:* SDI, spectral density of irradiance.

Studies and models of processes that control human circadian activities have not considered the combined action of circadian and 11-year cyclic variations of irradiance thus far.

This work presents a description of spectrally selective transformations performed by receivers of optical radiation in the pathway controlling circadian activities under the combined effect of circadian and 11-year variations in spectral and energetic indices of solar irradiance. This description is important for biology, chronobiology, and light engineering.

Solar radiation acts on the analog receivers of optical radiation, which are a system of blue-sensitive cones (S cones) and rods that are located in peripheral areas of the retina [5]. Rods and S cones are the initial step in the pathway that controls human circadian activity [1]. At this step, the circadian activity control pathway receives solar radiation and performs its spectrally selective processing. This processing includes

the isolation of the circadian component of the solar radiation spectrum and supports the control of human circadian activity proper.

This processing generates neuron signals formed by retinal ganglion (output) cells. They bear binary information on the spectral density of irradiance (SDI), which has been received and processed by the analog receivers of optical radiation [5].

The output signals formed by retinal ganglion cells are transduced to the suprachiasmatic nuclei of the hypothalamus, where signals that control the circadian activity of the pineal gland, which secretes melatonin to blood plasma, are formed. The circadian changes in the blood plasma melatonin level ultimately control human circadian activities.

The binary retinal outputs signals form a bijective and bicontinuous homeomorphic map of the SDI acting on the retina. Therefore, for clarity and convenience, the transformations of signals in the circadian activities controlling pathway are described below via analog representations of binary signals with appropriate terms and concepts.

The  $m_{eS}(\lambda, T)$  function of the spectral density of the luminance of the photosphere of the Sun is described by Planck's law for a black body [6, 7]:

$$m_{eS}(\lambda, T) = C_1 \lambda^{-5} \left( \exp \frac{C_2}{\lambda T} - 1 \right)^{-1}, \quad (1)$$

where  $\lambda$  is the radiation wavelength;  $T$ , the absolute temperature of the equilibrium black body radiation;  $C_1 \approx 3.742 \times 10^{-16} \text{ W m}^2$ ; and  $C_2 \approx 1.439 \times 10^{-2} \text{ m K}$ .

The SDI at the normal incidence of solar radiation on an area at the upper boundary of the terrestrial atmosphere is

$$\begin{aligned} e_{eS}(\lambda, T_{\text{eff}}) &= \left( \frac{r}{R} \right)^2 m_{eS}(\lambda, T_{\text{eff}}) \\ &= \left( \frac{r}{R} \right)^2 C_1 \lambda^{-5} \left( \exp \frac{C_2}{\lambda T_{\text{eff}}} - 1 \right)^{-1}, \end{aligned} \quad (2)$$

where  $T_{\text{eff}}$  is the effective (averaged over the photosphere) absolute temperature of the solar radiation,  $r = 6.96 \times 10^5 \text{ km}$  is the Sun's equatorial radius, and  $R = 1.496 \times 10^{12} \text{ km}$  is the radius of the Earth's circular orbit [8, 9].

According to the recommendations of the International Radiation Commission [10],  $T_{\text{eff}}$  is taken to be constant; this does not allow the dependence of  $e_{eS}(\lambda, T_{\text{eff}})$  on the year number within a solar cycle to be constructed.

Obviously, in Eq. (2)  $T_{\text{eff}} = T_{\text{eff}}(n)$ . To determine the  $T_{\text{eff}}(n)$  function, we applied the solar constant SC (Eq. (3)), which is the irradiance of an area at the upper boundary of the terrestrial atmosphere at the normal incidence of solar radiation [11].

$$\begin{aligned} E_{\text{SC}}(T_{\text{eff}}) &= \int_0^{\infty} e_{eS}(\lambda, T_{\text{eff}}) d\lambda \\ &= \left( \frac{r}{R} \right)^2 \int_0^{\infty} m_{eS}(\lambda, T_{\text{eff}}) d\lambda. \end{aligned} \quad (3)$$

Satellite solar radiometrical measurements of the maximum values of the 20th and 21st solar activity cycles [2–4] indicate that the most probable  $E_{\text{SC}}(T_{\text{eff}})$  value is within 1368–1377  $\text{W/m}^2$ , with the time variation of this index being irregular. Therefore, the term *solar constant* is used. The standard solar constant value, which corresponds to the maximum solar activity, is taken to be  $E_{\text{SC}, \text{max}}(T_{\text{eff}}) \approx 1370 \text{ W/m}^2$ , in accordance with the International Pyrheliometric Scale [9, 10]. As follows from Eqs. (2) and (3), this  $E_{\text{SC}, \text{max}}(T_{\text{eff}})$  value corresponds to  $T_{\text{eff}, \text{max}} = 5780 \text{ K}$ .

The  $T_{\text{eff}, \text{min}}$  and  $E_{\text{SC}, \text{min}}$  values were calculated by invoking the so-called light solar constant  $E_{\text{LSC}, \text{min}}(T_{\text{eff}})$  within the wavelength range  $350 \times 10^{-9} \leq \lambda \leq 770 \times 10^{-9} \text{ m}$ :

$$\begin{aligned} E_{\text{LSC}}(T_{\text{eff}}) &= 683 \int_{350 \times 10^{-9}}^{770 \times 10^{-9}} e_{eS}[\lambda, T_{\text{eff}} V(\lambda)] d\lambda \\ &= \left( \frac{r}{R} \right)^2 \times 683 \int_{350 \times 10^{-9}}^{770 \times 10^{-9}} m_{eS}[\lambda, T_{\text{eff}}] V(\lambda) d\lambda, \end{aligned} \quad (4)$$

which is the illuminance of an area at the upper boundary of the terrestrial atmosphere at the normal incidence of the solar radiation at the minimum solar activity. At the minimum solar activity,  $E_{\text{LSC}, \text{min}} = 135110 \text{ lx}$  [12]. It follows from Eqs. (2) and (4) that this  $E_{\text{LSC}, \text{min}}$  value corresponds to  $E_{\text{SC}, \text{min}} = 1106 \text{ W/m}^2$  and  $T_{\text{eff}, \text{min}} = 5480 \text{ K}$ .

The above indices for the maximum solar activity ( $E_{\text{SC}, \text{max}}(T_{\text{eff}}) \approx 1370 \text{ W/m}^2$  and  $T_{\text{eff}, \text{max}} = 5780 \text{ K}$ ) correspond to the light solar constant value  $E_{\text{LSC}} = 173600 \text{ lx}$ .

The variation of the effective absolute temperature of the Sun's photosphere radiation  $T_{\text{eff}}(n)$  at the above  $T_{\text{eff}, \text{min}}$  and  $T_{\text{eff}, \text{max}}$  values within an arbitrary solar cycle, whose temporal indices are obtained by averaging of the 25 known solar activity cycles [2–4], is described as

$$T_{\text{eff}}(n) = T_{\text{eff}, \text{avg}} \left[ 1 + 0.027 \sin \left( \frac{2\pi n}{11} - \frac{\pi}{2} \right) \right], \quad (5)$$

where  $T_{\text{eff}, \text{avg}} = 0.5(T_{\text{eff}, \text{min}} + T_{\text{eff}, \text{max}})$ .

Equation (5) is plotted in Fig. 1.

The minimum and maximum values of the so-called solar and light solar constants in various wavelength ranges are shown in Table 1.

The  $E_{\text{SC}}$  dependences deduced from Eq. (3) at  $E_{\text{SC}, \text{min}}$  and  $E_{\text{SC}, \text{max}}$  values calculated for the wave-

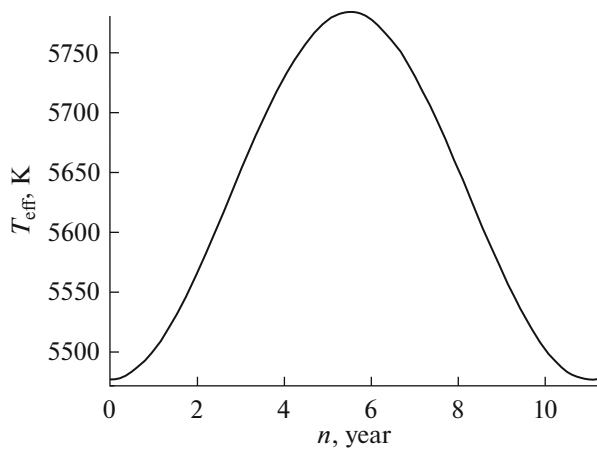


**Fig. 1.** The variation of the effective absolute temperature of the radiation of the Sun's photosphere within an 11-year solar cycle.

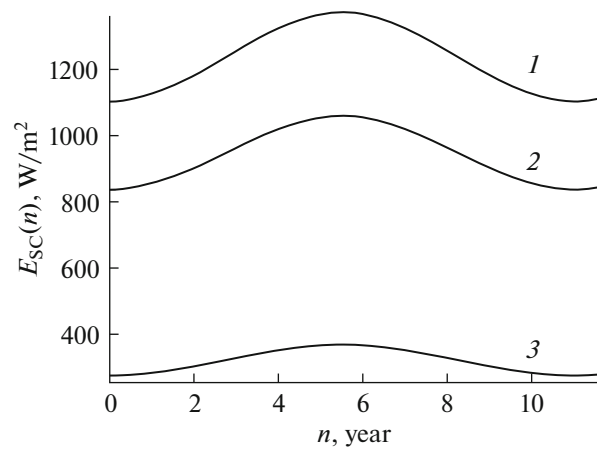


**Fig. 2.** The variation of the solar constant in various spectral ranges (nm) of solar radiation in an arbitrary solar cycle: (1)  $0 \leq \lambda \leq \infty$ ; (2)  $300 \leq \lambda \leq 1200$ ; (3)  $350 \leq \lambda \leq 770$ .

length range  $0 \leq \lambda \leq \infty$  nm, the atmospheric spectral window  $300 \leq \lambda \leq 1200$  nm, and the circadian spectral range  $350 \leq \lambda \leq 570$  nm are:

$$E_{SC}(n) = E_{SC, \text{avg}} \left[ 1 + 0.1062 \sin \left( \frac{2\pi n}{11} - \frac{\pi}{2} \right) \right], \quad (6)$$

at  $0 \leq \lambda \leq \infty$  nm,

$$E_{SC}(n) = E_{SC, \text{avg}} \left[ 1 + 0.1153 \sin \left( \frac{2\pi n}{11} - \frac{\pi}{2} \right) \right], \quad (7)$$

at  $300 \leq \lambda \leq 1200$  nm, and

$$E_{SC}(n) = E_{SC, \text{avg}} \left[ 1 + 0.1485 \sin \left( \frac{2\pi n}{11} - \frac{\pi}{2} \right) \right], \quad (8)$$

at  $350 \leq \lambda \leq 570$  nm.

The  $E_{SC, \text{avg}}$  values for each spectral range are shown in the bottom row of Table 1. The plots of Eqs. (6)–(8) are shown in Fig. 2.

Solar radiation that has passed through the atmosphere has direct and diffuse components. The direct  $e_{\text{Dir}, eS}(\lambda, h)$  and diffuse  $e_{\text{Dif}, eS}(\lambda, h)$  components of SDI after the propagation in the atmospheric spectral window are described as

$$\begin{aligned} & e_{\text{Dir}, eS}[\lambda, T_{\text{eff}, \text{Dir}}(h)] \\ &= \left( \frac{r}{R} \right)^2 m_{eS}[\lambda, T_{\text{eff}, \text{Dir}}(h)] \tau_{\text{Dir}}(h), \end{aligned} \quad (9)$$

$$\begin{aligned} & e_{\text{Dif}, eS}[\lambda, T_{\text{eff}, \text{Dif}}(h)] \\ &= \left( \frac{r}{R} \right)^2 m_{eS}[\lambda, T_{\text{eff}, \text{Dif}}(h)] \tau_{\text{Dif}}(h), \end{aligned} \quad (10)$$

where  $\tau_{\text{Dir}}(h)$  and  $\tau_{\text{Dif}}(h)$  are the dependences of the integral atmospheric transmission coefficients for the direct and diffuse components of solar radiation on the Sun's elevation in the spectral window of the Earth's atmosphere of  $300 \leq \lambda \leq 1200$  nm.

Obviously, the types of the  $\tau_{\text{Dir}}(h)$  and  $\tau_{\text{Dif}}(h)$  functions depend significantly on the current state of the atmosphere and are determined by the presence or absence of clouds and by their quantity.

The  $\tau_{\text{Dir}}(h)$  and  $\tau_{\text{Dif}}(h)$  functions used below were deduced from experimental data [12]. The data presented by Sharonov [12] are the most complete corpus of knowledge that permit one to construct the dependences of illuminance and irradiation of the Earth's surface on the Sun's elevation.

**Table 1.** The values of the solar constant  $E_{SC}$  in various spectral ranges and light solar constant  $E_{LSC}$  values in the visible spectral range at the maximum and minimum solar activities.

Solar activity type	$E_{SC}, \text{W/m}^2$ at $0 \leq \lambda \leq \infty$ nm	$E_{SC}, \text{W/m}^2$ at $300 \leq \lambda \leq 1200$ nm (atmospheric spectral window) [13])	$E_{SC}, \text{W/m}^2$ at $350 \leq \lambda \leq 570$ nm (circadian spectral range)	$E_{LSC}, \text{lx}$ , at $350 \leq \lambda \leq 770$ nm (visible spectral range)
Minimum	1106.3	838.7	272.6	135110
Maximum	1369.2	1057.4	367.7	173600
Averaged	1237.7	948.1	320.1	154355

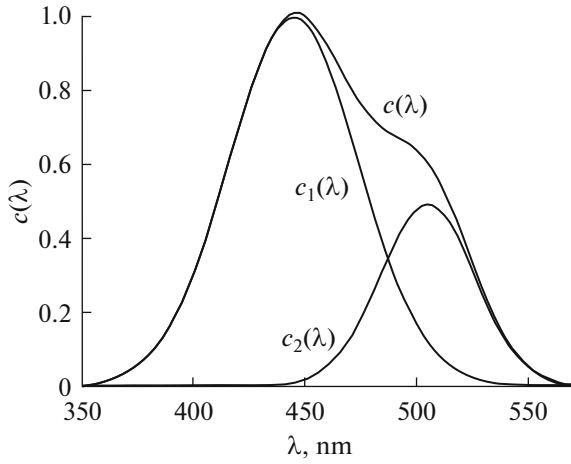


**Fig. 3.** Plots of the relative spectral circadian efficiency:  $c_1(\lambda)$ ;  $c_2(\lambda)$ ;  $c(\lambda)$ .

We consider the case of a cloudless sky as an example. In this case, the  $\tau_{\text{Dir}}(h)$  and  $\tau_{\text{Dif}}(h)$  functions are described as follows:

$$\tau_{\text{Dir}}(h) = \tau_{\text{Dir}}(90^\circ) \times 0.5[1 + \sin(0.035h - 1.47)], \quad (11)$$

$$\tau_{\text{Dif}}(h) = \tau_{\text{Dif}}(90^\circ) \times 0.5[1 + \sin(0.029h - 1.09)]. \quad (12)$$

$$e_{\text{Dir}, eS}(\lambda, h, n) = \left(\frac{r}{R}\right)^2 C_1 \lambda^{-5} \left\{ \exp \frac{C_2}{\lambda \left[ -3780 \exp(-0.2444h) + 5630 \left[ 1 + 0.027 \sin\left(\frac{2\pi n}{11} - \frac{\pi}{2}\right) \right] \right]} - 1 \right\}^{-1} \times 0.729 \times 0.5[1 + \sin(0.035h - 1.47)], \quad (15)$$

$$e_{\text{Dif}, eS}(\lambda, h, n) = \left(\frac{r}{R}\right)^2 C_1 \lambda^{-5} \left\{ \exp \frac{C_2}{\lambda \left[ 8950 \exp(-0.2084h) + 5630 \left[ 1 + 0.027 \sin\left(\frac{2\pi n}{11} - \frac{\pi}{2}\right) \right] \right]} - 1 \right\}^{-1} \times 0.205 \times 0.5[1 + \sin(0.029h - 1.09)]. \quad (16)$$

The values  $n = 0$  and  $n = 5.5$  in Eqs. (15) and (16) refer to the minimum and maximum solar activities, respectively. The differences between values of (15) at  $n = 0$  and  $n = 5.5$  and between values of (16) at  $n = 0$  and  $n = 5.5$  describe the maximum variations of SDI  $e_{\text{Dir}, eS}(\lambda, h)$  and  $e_{\text{Dif}, eS}(\lambda, h)$  on the Earth's surface within a single solar cycle.

The solar radiation that reaches the Earth's surface and is described by the SDIs of the direct and diffuse components (Eqs. (15) and (16)) or their sum acts on the S cones and rods of the retina. These light receivers process the radiation in a spectrally selective manner by the relative spectral circadian efficiency function  $c(\lambda)$  [5], which has been deduced from results of independent experiments [15–17]. The  $c(\lambda)$  function can be presented as the normalized sum of weighted func-

In Eqs. (11) and (12), the values  $\tau_{\text{Dir}}(90^\circ)$  and  $\tau_{\text{Dif}}(90^\circ)$  are the integral coefficients of atmospheric light transmission with a cloudless sky at the equator with the normal incidence of solar radiation on the Earth's surface on the days of the March or September equinox.

The circadian dependences of the direct  $T_{\text{Dir}}(h)$  and diffuse  $T_{\text{Dif}}(h)$  components of the absolute temperature of solar radiation on the Earth's surface with regard to the 11-year solar cycle are:

$$T_{\text{eff, Dir}}(h, n) = [-3780 \exp(-0.2444h) + T_{\text{eff}}(n)], \quad (13)$$

$$T_{\text{eff, Dif}}(h, n) = [8950 \exp(-0.2084h) + T_{\text{eff}}(n)]. \quad (14)$$

The first terms in Eqs. (13) and (14) are the dependences of the absolute temperatures of the direct and diffuse components of solar radiation on the Earth's surface in the daytime of an arbitrary day of the year as determined from independent experimental data. The second terms are described by Eq. (5).

By substituting expressions (13) and (14) and numerical values of  $\tau_{\text{Dir}}(90^\circ)$  and  $\tau_{\text{Dif}}(90^\circ)$  to Eqs. (9) and (10), we obtain the formulas for the dependences of SDI of the direct  $e_{\text{Dir}, eS}(\lambda, h, n)$  and diffuse  $e_{\text{Dif}, eS}(\lambda, h, n)$  components of solar radiation on wavelength  $\lambda$  in the atmospheric spectral window and on the Sun's elevation at any point of the Earth's surface at a certain  $n$  in the solar cycle:

tions of relative spectral sensitivity of S cones ( $c_1(\lambda)$ ) and rods ( $c_2(\lambda)$ ) [5]:

$$c(\lambda) = c_1(\lambda) + c_2(\lambda) = \frac{\alpha_1}{\sigma_1 \sqrt{2\pi}} \exp \left[ -\frac{(\lambda - \lambda_{1, \text{max}})^2}{2\sigma_1^2} \right] + \frac{\alpha_2}{\sigma_2 \sqrt{2\pi}} \exp \left[ -\frac{(\lambda - \lambda_{2, \text{max}})^2}{2\sigma_2^2} \right], \quad (17)$$

where  $\alpha_1 = 72.56$  nm,  $\sigma_1 = 28.99$  nm,  $\lambda_{1, \text{max}} = 445$  nm,  $\alpha_2 = 25.89$  nm,  $\sigma_2 = 21.21$  nm,  $\lambda_{2, \text{max}} = 505$  nm.

This function is plotted in Fig. 3.

The analog representations of binary signals formed by retinal ganglion cells depend on the Sun's elevation. They are expressed as a product in which the multiplicand is the direct  $e_{\text{Dir}, eS}(\lambda, h, n)$ , or diffuse

$e_{\text{Dir}, eS}(\lambda, h, n)$  component of solar radiation, or their sum, and the multiplier is the relative spectral circadian efficiency factor  $c(\lambda)$ . The  $c(\lambda)$  function, as well as its terms  $c_1(\lambda)$  and  $c_2(\lambda)$ , can be treated as characteristics of light filters that isolate narrow bands in the spectral ranges of their domains from the broadband solar radiation (within the atmospheric spectral window). These functions thus perform the narrow-band spectral selection of solar radiation [18].

Obviously, in the actual control of human circadian activities by solar radiation retinal S cones and rods are most exposed to the sum of the direct  $e_{\text{Dir}, eS}(\lambda, h, n)$  and diffuse  $e_{\text{Dif}, eS}(\lambda, h, n)$  components. Normally, without catastrophic injuries of the fiber tracts from S cones and rods to hypothalamic supra-chiasmatic nuclei, the direct and diffuse components undergo spectral selection by the sum of functions  $c_1(\lambda)$  and  $c_2(\lambda)$ .

The variants of separate processing of the direct  $e_{\text{Dir}, eS}(\lambda, h, n)$  and diffuse  $e_{\text{Dif}, eS}(\lambda, h, n)$  SDI components by the functions  $c_1(\lambda)$  and  $c_2(\lambda)$  or their combinations are also of theoretical and practical interest.

In this case, we can compose the products  $e_{i, eS}(\lambda, h, n) \times c_j(\lambda)$  (the index  $i = 1, 2$  denotes the direct or diffuse SDI component, and  $j = 1, 2$  denotes  $c_1(\lambda)$  or  $c_2(\lambda)$ ), elucidate features of the separate processing of the direct  $e_{\text{Dir}, eS}(\lambda, h, n)$  and diffuse  $e_{\text{Dif}, eS}(\lambda, h, n)$  SDI components by the functions  $c_1(\lambda)$  and  $c_2(\lambda)$  or their sum, and describe various paths of

spectral selection of solar radiation in the control of human circadian activities.

The domains of the functions  $c_1(\lambda)$  and  $c_2(\lambda)$  are within  $350 \leq \lambda \leq 550$  nm and  $435 \leq \lambda \leq 570$  nm, respectively, and the domain of their sum is in the spectral range  $350 \leq \lambda \leq 570$  nm [5].

The spectral functions  $c_1(\lambda)$  and  $c_2(\lambda)$  form two overlapping spectral channels of solar radiation processing: short-wave and long-wave, respectively.

The variants of solar radiation processing with just one of the functions  $c_1(\lambda)$  or  $c_2(\lambda)$  describe the cases of catastrophic damage of the neuronal paths from rods and S cones, respectively, to hypothalamic supra-chiasmatic nuclei.

The weighting factors  $\alpha_1$  and  $\alpha_2$  in Eq. (17) do not vary with the Sun's elevation in the daytime [19]. It is obvious that the spectral characteristics of the functions  $c_1(\lambda)$  and  $c_2(\lambda)$ , as well as the spectral characteristics of the products  $e_{i, eS}(\lambda, h, n) \times c_j(\lambda)$  also remain constant, regardless of the  $\alpha_1$  and  $\alpha_2$  values. The absolute values of  $e_{i, eS}(\lambda, h, n) \times c_j(\lambda)$  still depend on the Sun's elevation.

In the most frequent case, when the sum of the direct and diffuse solar radiation components simultaneously act on the short- and long-wave spectral channels (Eqs. (15)–(17)), the equation for SDI formed by spectrally selective processing of solar radiation with the function  $c(\lambda) = c_1(\lambda) + c_2(\lambda)$  takes the form

$$\begin{aligned}
 e_{\text{Dir}+\text{Dif}, \text{SW}+\text{LW}}(\lambda, h, n) &= [e_{\text{Dir}, eS}(\lambda, h, n) + e_{\text{Dif}, eS}(\lambda, h, n)][c_1(\lambda) + c_2(\lambda)] \\
 &= \left(\frac{r}{R}\right)^2 C_1 \lambda^{-5} \left\{ \left[ \exp \frac{C_2}{\lambda[-3780 \exp(-0.2444h) + T_{\text{eff}}(n)]} - 1 \right]^{-1} \times 0.729 \times 0.5[1 + \sin(0.035h - 1.47)] \right\} \\
 &\quad + \left\{ \left[ \exp \frac{C_2}{\lambda[8950 \exp(-0.2084h) + T_{\text{eff}}(n)]} - 1 \right]^{-1} \times 0.205 \times 0.5[1 + \sin(0.029h - 1.09)] \right\} \\
 &\quad \times \left\{ \frac{\alpha_1}{\sigma_1 \sqrt{2\pi}} \exp \left[ -\frac{(\lambda - \lambda_{1\text{max}})^2}{2\sigma_1^2} \right] + \frac{\alpha_2}{\sigma_2 \sqrt{2\pi}} \exp \left[ -\frac{(\lambda - \lambda_{2\text{max}})^2}{2\sigma_2^2} \right] \right\}, \tag{18}
 \end{aligned}$$

where the function  $T_{\text{eff}}(n)$  is described by Eq. (5).

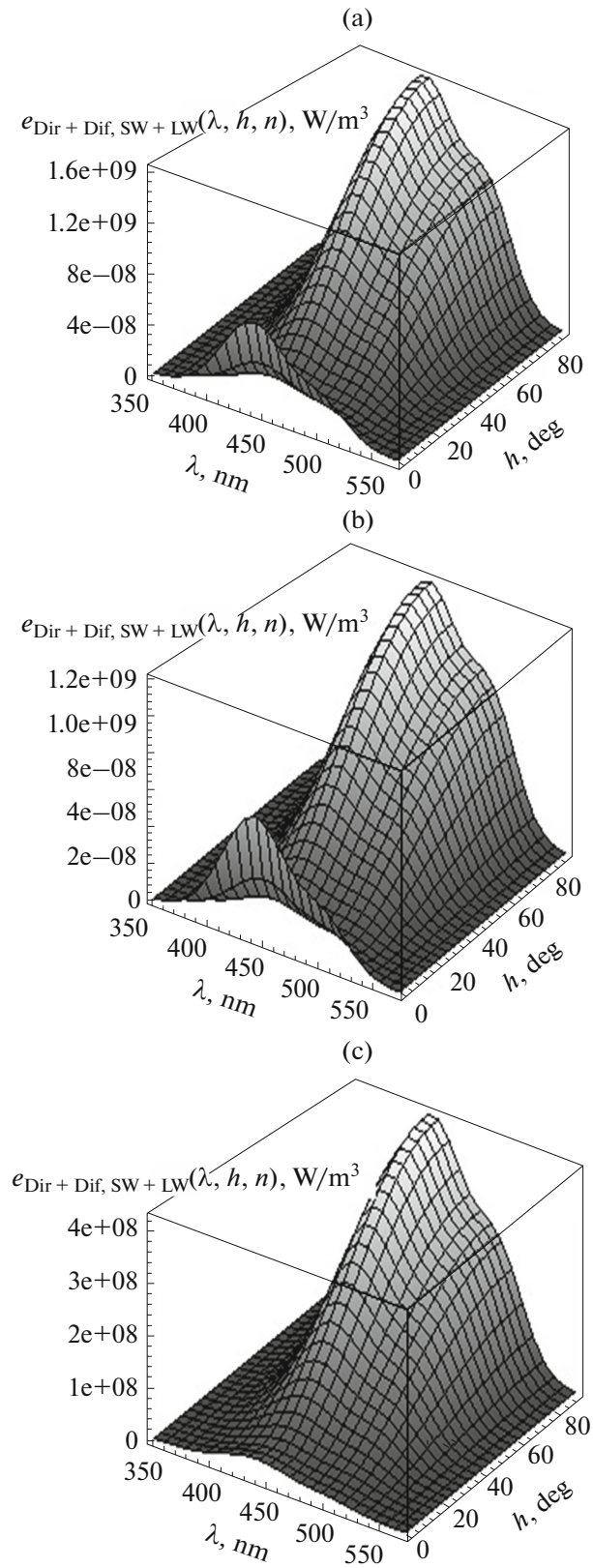
Various combinations of  $e_{\text{Dir}, eS}(\lambda, h, n)$ ,  $e_{\text{Dif}, eS}(\lambda, h, n)$ ,  $c_1(\lambda)$ , and  $c_2(\lambda)$  can be constructed by using Eq. (18). The equation also allows the description and analysis of features of spectrally selective solar radiation processing with various combinations of functions (14)–(16).

Figure 4 presents plots of Eq. (18) in the circadian range of solar radiation at the maximum and minimum solar activities ( $n = 5.5$ ,  $T_{\text{eff}} = 5780$  K and  $n = 0$ ,  $T_{\text{eff}} = 5480$  K, respectively) and a plot showing the differences between the absolute values of  $e_{\text{Dir}+\text{Dif}, \text{SW}+\text{LW}}(\lambda, h, n)$  at the maximum and minimum

solar activities obtained by spectrally selective processing of solar radiation by retinal rods and cones.

It immediately follows from Figs. 4a, 4b that the spectral characteristics of the functions  $e_{\text{Dir}, eS}(\lambda, h, n)$  and  $e_{\text{Dif}, eS}(\lambda, h, n)$  retain their shapes regardless of the Sun's elevation. In contrast, their energetic characteristics depend considerably on the wavelength of solar radiation in the circadian spectral range and on the current elevation of the Sun.

Figure 5 presents plots of the difference between SDI values at the maximum and minimum solar activities  $\Delta e_{\text{Dir}+\text{Dif}, \text{SW}+\text{LW}}(\lambda, h, n)$  at the wavelength  $\lambda = 445$  nm and of the difference between SDI values taken relative to SDI at the minimum solar activity



**Fig. 4.** The dependence of the spectral density of illuminance on the Sun's angular elevation and radiation wavelength, formed by the sum of the direct and diffuse solar radiation components at the simultaneous action on the short- and long-wave spectral channels: (a) at the maximum solar activity ( $n = 5.5$ ;  $T_{\text{eff}} = 5780$  K); (b) at the minimum solar activity ( $n = 0$ ,  $T_{\text{eff}} = 5480$  K). (c) The difference between the SDIs at the maximum and minimum solar activity.

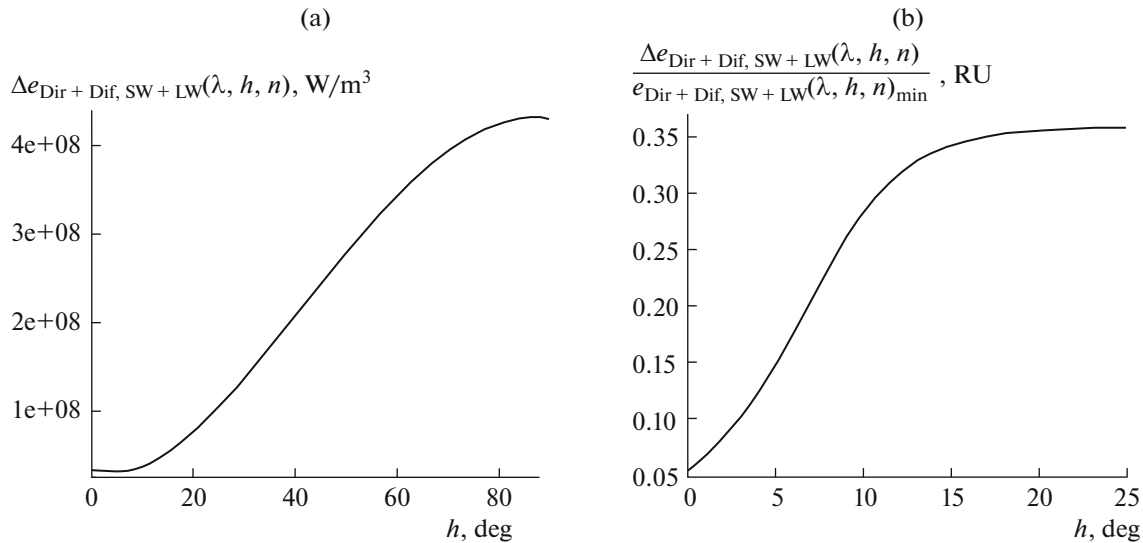


**Fig. 5.** (a) The variation of the SDI difference at  $\lambda = 445 \text{ nm}$  with the Sun's elevation  $h$  from  $0^\circ$  to  $90^\circ$ . (b) Variation of the SDI difference taken relative to SDI at the minimum solar activity.

$\frac{\Delta e_{\text{Dir} + \text{Dif}, \text{SW} + \text{LW}}(\lambda, h, n)}{e_{\text{Dir} + \text{Dif}, \text{SW} + \text{LW}}(\lambda, h, n)_{\text{min}}}$  with the Sun's elevation  $h$  varying from  $0^\circ$  to  $90^\circ$ .

The maximum value of the SDI difference in the circadian range of the solar emission spectrum at the maximum and minimum solar activities at  $\lambda = 445 \text{ nm}$ ,  $h = 90^\circ$  is  $4.302 \times 10^8 \text{ W/m}^3$ .

It follows from Fig. 5b that the relative SDI differences at the maximum and minimum solar activities occur at small elevations of the Sun and range from 5 to 36%. This value reaches the plateau of 36% at the elevations of the Sun of  $h > 25^\circ$ .

By using this method, explicit expressions that describe the integral transmission coefficients of the Earth's atmosphere and the spectrally selective processing of solar radiation that controls human circadian activities with various types and percentages of the cloud canopy can be obtained in a similar way from the data reported in [12].

This analysis indicates that the circadian activity component in the spectrum of any broad-band source of optical radiation is determined solely by the spectral-selective properties of rods and S cones. However, in this case the use factor of broad-band radiation is too low. This factor can be improved by utilizing specialized lighting systems designed for the prevention and/or mitigation of disturbances of human circadian activities. Such systems should employ narrow-band sources of optical radiation with overall radiation spectra corresponding to the spectral range of human circadian activity  $350 \leq \lambda \leq 570 \text{ nm}$ .

These results indicate that biological, chronobiological, and light-engineering studies of diurnal variations should take the 11-year solar optical activity cycle into consideration. In particular, experimental and theoretical studies of circadian activities and the modeling of control of human circadian activities by solar radiation would allow correct interpretation of the results and proper inferences.

## REFERENCES

1. A. V. Leonidov, *Biophysics (Moscow)* **59** (4), 658 (2014).
2. Yu. I. Vitinskii, M. Kopetskii, and G. V. Kuklin, *Statistics of the Solar Spot Activity* (Nauka, Moscow, 1986) [in Russian].
3. <http://www.sidc.be/silso/ssngraphics> (SILSO data/image, Royal Observatory of Belgium, Brussels).
4. [http://cyclowiki.org/wiki/11-letnii\\_tsikl\\_solnechnoi\\_aktivnosti](http://cyclowiki.org/wiki/11-letnii_tsikl_solnechnoi_aktivnosti).
5. A. V. Leonidov, *Biophysics (Moscow)* **61** (6), 1002 (2016).
6. R. M. Gagliardi and Sh. Karp, *Optical Communications* (Wiley, New York, 1976; Svyaz' Moscow, 1978).
7. E. G. Pestov and G. M. Lapshin, *Quantum Electronics* (Voenizdat, Moscow, 1972) [in Russian].
8. *Alpha and Omega: A Concise Handbook*, 2nd ed. (Valgus, Tallin, 1988) [in Russian].
9. C. W. Allen, *Astrophysical Quantities*, 3rd ed. (Athlone, London, 1975; Mir, Moscow, 1977).
10. A. A. Kmito and Yu. A. Sklyarov, *Pyreheliometry* (Gidrometeoizdat, Leningrad, 1981) [in Russian].
11. *Space Physics: A Concise Encyclopedia*, Ed. by R. A. Syunyaev (Sovetskaya Entsiklopediya, Moscow, 1986) [in Russian].

12. V. V. Sharonov, *Tables for Calculation of Natural Illuminance and Visibility* (Akad. Nauk SSSR, 1945) [in Russian].
13. E. V. Kononovich and V. I. Moroz, *A Course in General Astronomy*, Ed. by V. V. Ivanov (Editorial URSS, Moscow, 2004) [in Russian].
14. K. Shvartser, *Color-controlled Lightng: Analysis and Optimization of Control Systems. Final Report* (2006). [http://www/bocom.eu/rus/catalog/downloads/Farblicht-stadie\\_rus.pdf](http://www/bocom.eu/rus/catalog/downloads/Farblicht-stadie_rus.pdf).
15. G. K. Breinard and G. L. Glikman, *Svetotekhnika*, No. 1, 4 (2004).
16. K. Thapan, J. Arendt, and D. J. Skene, *J. Physiol.* **535**, 261 (2001).
17. G. C. Brainard and I. Provencio, in *2nd CIE Expert Symp. "Lighting and Health" CIE 031* (2006).
18. A. V. Leonidov and V. G. Baryshnikov, *Svetotekhnika*, No. 5, 12 (1983).
19. A. V. Leonidov, *Svetotekhnika*, No. 2, 66 (2012).

*Translated by Victor Gulevich*